FEMS Microbes, 2025, **6**, xtaf001
DOI: 10.1093/femsmc/xtaf001
Advance access publication date: 3 February 2025
Research Article – Microbes & Disease

Influenza a virus subtype H9N2 infection induces respiratory microbiota dysbiosis in chickens via type-I interferon-mediated mechanisms

Samson Oladokun[1,2], Mohammadali Alizadeh[1], Amirul I. Mallick[3], Fatemeh Fazel[1], Janan Shoja Doost[1], Katherine Blake[1], Myles St Denis[1], Sugandha Raj[1], Shayan Sharif[1,*]

[1]Department of Pathobiology, Ontario Veterinary College, University of Guelph, Guelph, ON N1G 2W1, Canada
[2]Present address: Department of Poultry Science, Texas A&M University, College Station, TX 77843, United States
[3]Department of Biological Sciences, Indian Institute of Science Education and Research Kolkata, Mohanpur, Nadia 741246, India
*Corresponding author. Department of Pathobiology, Ontario Veterinary College, University of Guelph, Guelph, ON N1G 2W1, Canada. E-mail: shayan@uoguelph.ca
Editor: [Daniel Weinberger]

Abstract

Avian influenza virus (AIV) poses significant threats to poultry and human health. This study investigates the impact of H9N2 AIV infection on the respiratory microbiota of chickens using 16S rRNA gene sequencing. Total 48 one-day-old specific pathogen-free chickens were assigned to six groups: a control and five post-infection groups (days 1, 3, 5, 7, and 9). After a 15-day microbiota stabilization period, the infected chickens received a viral inoculum (10^7 TCID50/ml) via ocular, intra-nasal, and intra-tracheal routes. Tracheal and broncho-alveolar lavage samples were analyzed. Significant reductions in microbiota diversity were observed on days 5, 7, and 9 post-infection, compared to d0 controls. Permutational Multivariate Analysis of Variance confirmed significant beta diversity differences ($P = 0.001$) between infected and uninfected groups. The microbial shifts from d5 to d9 were marked by increased Proteobacteria, decreased Actinobacteria and Firmicutes, and a rise in Dickeya. Elevated type-I interferon (IFN-β) and viperin gene expression at d5 coincided with reduced microbiota diversity, highlighting the respiratory microbiota's role in modulating host responses to AIV H9N2 infection and suggesting potential biomarkers for respiratory dysbiosis.

Keywords: avian influenza; respiratory tract; microbiota; dysbiosis; type-I interferon; biomarkers

Introduction

Avian influenza viruses (AIVs) are zoonotic pathogens that pose significant threats to both poultry and potentially human health (Cardona et al. 2009). These viruses are responsible for respiratory infections in poultry, which frequently lead to high morbidity and mortality rates, as well as decreased egg production. Based on pathogenicity, there are two major AIV pathotypes: highly pathogenic avian influenza viruses **(**HPAIs) such as H5N1, and low pathogenic avian influenza viruses (LPAIs), such as H9N2 (Pantin-Jackwood and Swayne 2009). HPAIs exhibit a mortality rate of 75% or greater in experimentally infected chickens and can cause 100% mortality in infected poultry within 48 h (WHO 2007, Suarez 2010). The clinical signs of AIV infection vary based on pathotypes, ranging from mild clinical signs such as lethargy, diarrhea, coughing, sneezing, and mild respiratory distress in LPAI-infected hosts, to severe clinical outcomes such as bleeding from the nares, incoordination, and even death in HPAI-infected hosts (Pantin-Jackwood and Swayne 2009, Chrzastek et al. 2021). AIV H9N2 infections have been documented in various poultry species, including domestic ducks, turkeys, and chickens in multiple countries since the mid-1990s, and are recently believed to have reached panzootic proportions (Nagy et al. 2017). Although the H9N2 AIV virus is classified as low pathogenicity, it still poses significant risks to both poultry and human health. This risk is amplified by its role in the genetic evolution of more virulent strains. For instance, the H5N2 AIV (A/chicken/Hebei/1102/2010), known for its high pathogenicity in chickens, acquired its internal gene cassette from H9N2 (Zhao et al. 2012). Additionally, the H9N2 virus has contributed to the evolution of other dangerous strains, such as H7N9, which has caused severe human disease. H7N9 acquired internal genes, including PB2 and PA, from H9N2, leading to mutations that enhance its transmissibility and pathogenicity (Huang and Wang 2020, Pu et al. 2021). This highlights H9N2's role in increasing the pathogenic potential of AIVs.

AIV primarily replicates in the epithelial cells of the gastrointestinal and respiratory tracts, which host a complex microbial community known as the microbiota, and often serve as an informative index for overall health status (Taylor et al. 2020). For example, the composition of the respiratory microbiota influence host immunocompetence through various mechanisms, including inflammatory responses, and colonization resistance via production of antimicrobial substances, competition for nutrients and attachment sites (Abt et al. 2012, Poroyko et al. 2015, Man et al. 2017). Virus infections can also induce broad or site-specific in host commensal microbiota (Yitbarek et al. 2018a, Zhao et al. 2018). The host's inflammatory response and gene expression, particularly type-I interferons (IFNs), are crucial in driving shifts in microbial community structure (Deriu et al. 2016). Type-I IFNs, including multiple IFN-α proteins and a single IFN-β protein, play a central role in antiviral defenses in chickens (Santhakumar et

Received 10 May 2024; **revised** 10 December 2024; **accepted** 2 February 2025

al. 2017). Any quantitative or qualitative disruption to the host's microbial homeostasis, also known as microbial dysbiosis, can potentially compromise the host's immunocompetence. Various environmental and pathogenic stressors can trigger microbial dysbiosis (Yitbarek et al. 2018a, Rostagno 2020). Epidemiological studies in humans have associated microbial dysbiosis with respiratory disorders such as airway inflammation, asthma, and chronic obstructive pulmonary disease (Russel et al. 2012, Rutten et al. 2014). Although research on the avian respiratory microbiota is limited, there has been extensive study of gut microbiota in poultry species. Several studies (Yitbarek et al. 2018a, Li et al. 2018, 2018b,c) have demonstrated the role of gut microbiota in viral pathogenesis. In particular, Yitbarek et al. (2018a) established an association between H9N2 AIV infection and gut microbiota dysbiosis by investigating the relationship between the gut microbiota and AIV in the chicken model.

Considering that the respiratory tract serves as the primary portal point for AIV entry and replication sites, we hypothesized that influenza A virus infection could alter the resident microbiota in the chicken respiratory tract. Such alterations could significantly impact the host innate immune defense and susceptibility to other infections. Thus, insights gained from such an investigation could inform future disease prevention and treatment strategies. Despite the advancements in sequencing technologies, there remains a dearth of information regarding how acute viral infections affect the composition, kinetics, and quantity of commensal microbiota in the chicken respiratory tract. The present study utilized 16S ribosomal RNA (16S rRNA) gene sequencing to examine the microbiota in the trachea and broncho-alveolar lavage (BAL), representing the upper respiratory tract (URT) and lower respiratory tract (LRT) of chickens, respectively, following infection with H9N2 influenza A virus.

Materials and methods

Experimental design

All experimental procedures received approval from the University of Guelph Animal Care Committee (AUP 5073) and were conducted in strict compliance with the Canadian Council on Animal Care (CCAC) guidelines. The study involved 48 one-day-old specific pathogen-free chickens (Canadian Food Inspection Agency-CFIA, Ottawa Laboratory, Nepean, ON, Canada). These chickens were randomly assigned to six treatment groups, each consisting of 8 birds. The groups included one control group (uninfected chickens) and five experimental groups, corresponding to days 1, 3, 5, 7, and 9 post-H9N2 infection. Each treatment group was housed in separate cages within Horsfall units in a Biosafety Level II isolation facility at the University of Guelph, Ontario, Canada. Although, all treatment groups were kept separately in different cages, they were maintained under uniform environmental conditions and provided unrestricted access to an antibiotic-free diet and water. The experimental unit was defined as an individual cage. All chickens were given a 15-day period for microbiota stabilization before the H9N2 AIV infection and sampling was carried out.

Virus propagation and infection of chickens

Specific-pathogen-free eggs (CFIA, Ottawa Laboratory, Nepean, ON, Canada) underwent a 10-day incubation period at 37°C. Each egg was then inoculated with 4 hemagglutination units (4HA) of the H9N2 LPAIV strain, specifically A/TK/IT/13VIR1864-45/2013 [Istituto Zooprofilattico Spermentale delle Venezie (IZSVe), Legnaro, Padua, Italy], followed by an additional 72-h incubation at 37°C. Embryos were subjected to regular monitoring every 24 h, and any dead embryo was promptly disposed of. After the 72-h incubation period, the eggs were stored at 4°C overnight. Subsequently, allantoic fluid was collected, pooled, and centrifuged at 400 × *g* for 15 min. This collected fluid was then stored at –80°C until further use. Virus quantification was carried out by titrating the virus on Madin–Darby canine kidney (MDCK) cells, with titers calculated based on endpoint dilutions. These results were expressed as 50% tissue culture infectious dose (TCID50/ml) (Reed and Muench 1938). Chickens in the H9N2 infection group were infected with a virus inoculum containing 10^7 TCID50/ml and administered through a combination of ocular (80 μl/eye), intranasal (80 μl/nostril), and intra-tracheal (80 μl) routes.

Assessment of viral load and shedding

On days 1, 3, 5, 7, and 9 post-infection (pi), as well as on day 0 pre-infection, oral and cloacal swabs were collected from all chickens in each group. These swab samples were collected using 15 cm Puritan PurFlock Ultra sterile flocked collection devices (Gilford, Maine, USA). Collected Swabs were then placed in 1.5-ml microcentrifuge tubes containing transport medium composed of DMEM (Dulbecco's Modified Eagle's medium) supplemented with 0.5% BSA fraction V, 10 ml of penicillin (200 U/ml), 80 μg/ml of streptomycin, and 50 μg/ml of gentamycin. The samples were kept on ice throughout the collection process until further processing and storage at −80°C.

For virus load quantification, the swab samples were serially diluted onto an 80%–95% confluent monolayer of MDCK cells and subsequently incubated at 37°C for 72 h. The titer was determined by identifying the highest dilution that displayed a cytopathic effect (CPE) under the microscope. This determination was confirmed by conducting a hemagglutination test using 0.5% chicken blood. The virus load, expressed as TCID50/ml, was subsequently calculated using the Reed and Muench (1938) method.

Collection of tracheal swabs and BAL fluid

At each time point—day 0 (pre-infection), and days 1, 3, 5, 7, and 9 post-infection (pi)—samples were collected from 8 chickens per treatment group. Each treatment group was housed in separate cages, with each cage containing 8 birds. For tracheal swab samples, swabs (Puritan PurFlock, Maine, USA) were gently inserted into the trachea and moved back and forth at least five times before immersing them in 1 ml of 1× PBS (Wisent Inc., Saint-Jean-Baptiste, QC, Canada). In the case of BAL samples, 1 ml of 1× PBS was slowly flushed down a small tracheal slit, ∼3 cm from the bronchia, using pipettes attached to 10 ml syringes (BD, Franklin Lakes, NJ, USA). Subsequently, the PBS solution was withdrawn and transferred to 1.5 ml microcentrifuge tubes (MCT-150-Y, Axygen, Union City, CA, USA). All samples were collected and immediately transferred to the laboratory on ice.

DNA extraction and 16S rRNA gene sequencing

Microbial genomic DNA was extracted from each tracheal and BAL sample using the PureLink Microbiome DNA Purification Kit (Catalog Number A29790, Thermo Fisher Scientific, Waltham, MA, USA) following the manufacturer's instructions. DNA quality and concentration were assessed using a NanoDrop spectrophotometer (NanoDrop Technologies, Wilmington, DE). Extracted DNA samples (volume: 50 µl, concentration: 10–200 ng/µl) were subsequently sent to the Integrated Microbiome Resource (IMR) (http://imr.bio) for library preparation and se-

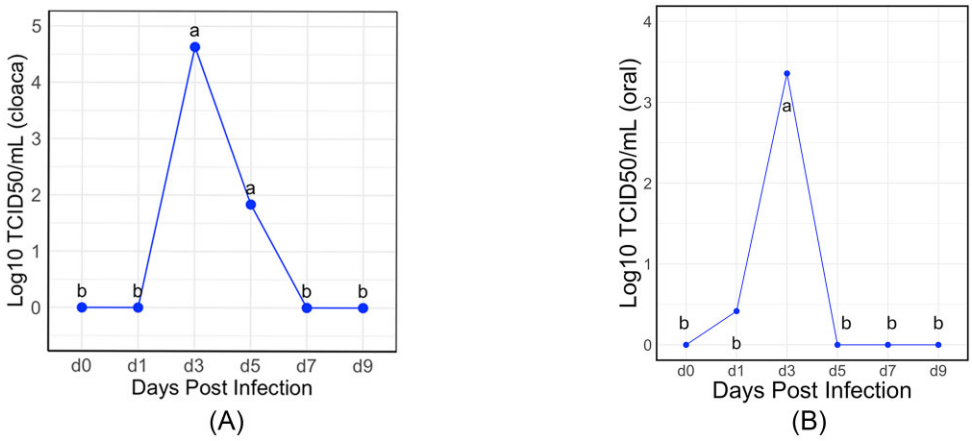

Figure 1. Oral and Cloacal H9N2 virus titer in chickens infected with 400 μl of 10^7 $TCID_{50}$/ml LPAI H9N2. Virus titer was determined at Days 0, 1, 3, 5, 7, and 9 post-infection using $TCID_{50}$ in MDCK cells.

quencing. Libraries targeting the V3–V4 hypervariable region of the 16S rRNA gene were PCR-amplified using dual-barcoded primers (341F = 5′-CCTACGGGNGGCWGCAG-3′ and 805R = 3′-GACTACHVGGGTATCTAATCC-5′).

RNA extraction, cDNA synthesis and real-time PCR

On days 1, 3, 5, 7, and 9 pi, as well as on day 0 pre-infection, tracheal tissues were collected from euthanized chickens ($n = 8$) in all groups. RNA extraction and cDNA synthesis followed established protocols using TRIzol® (Invitrogen, Invitrogen, Carlsbad, CA, USA) and Superscript® II First-Strand Synthesis kit (Invitrogen) (Barjesteh et al. 2015). Real-time PCR was conducted using diluted cDNA on the LightCycler® 480 II instrument (Roche Diagnostics GmbH, Mannheim, DE, Germany) employing the SyBR Green Mix from the same manufacturer. Primers were procured from Sigma–Aldrich in Oakville, Canada, with specific sequences provided in Supplementary Table S1 (Barjesteh et al. 2015; Boodhoo et al. 2023, Raj et al. 2023). Relative expression levels of target genes were normalized to the housekeeping gene β-actin and calculated using LightCycler® 480 II system (Roche Diagnostics GmbH, Mannheim, DE) (Alizadeh et al. 2020).

Statistical and bioinformatics analysis

All datasets were analyzed using the Minitab statistical package (v.18.1). Generalized linear models were applied to analyze non-viral datasets, with mean differences assessed using Tukey's Honest Significant Difference test. Viral shedding data were analyzed using repeated measures analysis of variance (ANOVA). The normality of the data was tested with the Shapiro–Wilk test. For data that did not follow a normal distribution, the Kruskal–Wallis test was used. Statistical significance was determined at a threshold of $P \leq 0.05$.

Bioinformatic analysis of microbiome data, including processing and filtering, followed the Microbiome Helper pipeline (Oladokun et al. 2022) using QIIME 2 (version 2023.7) software package. Rare ASVs were filtered out based on the criteria of being present in at least 1 sample and frequency of <0.1% of the mean sample depth (26 757 reads per sample). Additionally mitochondrial and chloroplast 16S sequences were filtered out as contaminants. PCR negative controls were included and sequenced on each plate in the run (4 per run) to identify potential contamination. These controls are generally not provided to clients by the sequencing core since they usually (as in the case of the runs in this paper) contain very little sequence content, primarily representing sequence bleedthrough on the MiSeqs (which is controlled for in Step 4.1 of the pipeline). Visualization was conducted using the MicrobiomeAnalyst 2.0 web-based platform (Lu et al. 2023). Individual alpha diversity was assessed via rarefaction curves, employing the default observed operational taxonomic unit (OTU) metric. Statistical significance of alpha diversity differences was determined using the Shannon index and assessed through Kruskal–Wallis test. Pearson correlation coefficient (r) was used to measure the strength and direction of the association between diversity metrics (Shannon diversity and beta diversity, assessed using PERMANOVA models) and viral metrics (viral load and shedding), as well as infection groups (days). Correlation analyses were performed in R (version 2024.04.2). Results were visualized using ggplot2, with bar plots representing Pearson's r values and color-coded *P*-values on a gradient from red (high *P*-value) to green (low *P*-value). Beta diversity was assessed using principal coordinates analysis (PCoA) plots based on weighted UniFrac distance matrices. Statistical significance of beta diversity differences was determined using Permutational Multivariate Analysis of Variance (PERMANOVA), considering only experimental factors (site- BAL or Tracheal swabs; days- d0, d1, d3, d5, d7, d9 pi) in the analysis. Relative abundances at various taxonomic levels were visualized using stacked bar charts. Significant microbiota proportions were identified using the Statistical Analysis of Metagenomic Profiles (STAMP v2.1.3) software (Parks et al. 2014).

Results

AIV H9N2 peak viral load and shedding confirmed at d3 pi

The virus load were assessed using $TCID_{50}$ method by titrating the oral and cloacal swab samples on MDCK cell monolayers. The AIV challenge model proved effective, with the peak AIV viral shedding occurring at d3 pi (Fig. 1). In oral swabs, viral load exhibited a gradual increase until d3 pi, thereafter, no cytopathic effects in the MDCK cells were observed in oral swabs. As for cloacal swabs, viral shedding was only detected beginning at d3 pi, followed by a 61% reduction in shedding at d5 pi. No cytopathic effects in the MDCK cells were observed in cloacal swabs after d5 pi. Control chickens (day 0 pre-infection group) were confirmed to be negative for the virus in both samples.

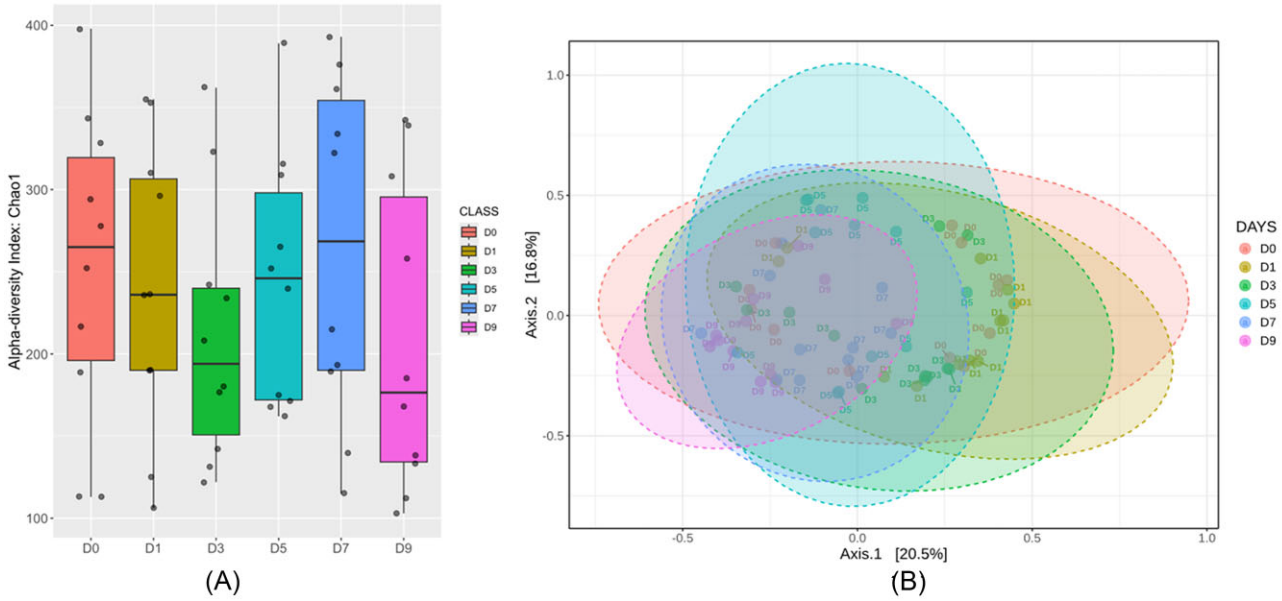

Figure 2. (A) Alpha diversity (Shannon index) box plots indicate significant difference ($P < 0.001$) between H9N2-infected chickens at days 0, 1, 3, 5, 7, and 9 post-infection and (B) PCoA plots based on weighted UniFrac metric illustrating the respiratory microbiota beta diversity. The comparisons conducted include H9N2-infected chickens at days 0, 1, 3, 5, 7, and 9 post-infection (PERMANOVA *F*-value: 7.1365; R-squared: 0.35092; *P*-value: 0.001). Samples were collected before challenge (day 0) and days 1, 3, 5, 7, and 9 post infection in chickens that were infected with 400 μl of 10^7 $TCID_{50}$/ml of H9N2 influenza virus.

Table 1. Post-hoc comparisons of alpha diversity (Shannon index) between control (D0) and Avian influenza H9N2-infected groups.

Comparisons	*P*-value	FDR-adjusted *P*-value
D0 vs D5	$7.209E^{-4}$	0.0015
D0 vs D1	0.5159	0.7455
D0 vs D3	0.8267	0.8267
D0 vs D7	$1.5878E^{-4}$	$5.9544E^{-4}$
D0 vs D9	$1.6786E^{-5}$	$1.5968E^{-4}$

This table presents results from pairwise comparisons of Shannon diversity indices, with multiple comparisons adjusted using the Benjamini–Hochberg procedure (FDR). Samples were collected from chickens before challenge (day 0) and at days 1, 3, 5, 7, and 9 post-infection. Chickens were inoculated with 400 μl of 10^7 TCID50/ml H9N2 influenza virus. Samples included broncho-alveolar lavage (BAL) and tracheal swabs. Significance was defined as $P \leq 0.05$.

Table 2. Permutational Multivariate Analysis of Variance (PERMANOVA) comparisons between control (D0) and Avian Influenza H9N2-infected groups.

Comparisons	*P*-value	FDR-adjusted *P*-value
D0 vs D5	0.3200	0.0017
D0 vs D1	0.0750	0.0900
D0 vs D3	0.0987	0.0330
D0 vs D7	0.3203	0.0017
D0 vs D9	0.4130	0.0017

This table presents results from pairwise Permutational Multivariate Analysis of Variance (PERMANOVA) analyses, with multiple testing adjustments applied using the Benjamini-Hochberg procedure (FDR). Samples were collected from chickens before challenge (Day 0) and at Days 1, 3, 5, 7, and 9 post-infection. Chickens were inoculated with 400 μl of 10^7 TCID50/ml H9N2 influenza virus. Samples included BAL and tracheal swabs. Significance was defined as $P \leq 0.05$.

AIV H9N2 infection induces spatial and temporal reduction in microbiota diversity.

Alpha diversity, as measured by the Shannon index, showed a significant reduction in microbiota diversity on Days 5, 7, and 9 post-infection with AIV compared to uninfected controls (d0). The lowest reduction ($P < 0.001$) was observed on d5 pi (Fig. 2A, Table 1, Supplementary Table S2 and S3). Similarly, BAL samples recorded a lower ($P = 0.02$) Shannon index compared to tracheal swab samples and distinct clustering patterns in beta diversity analysis, based on weighted UniFrac distances (Supplementary Fig. S1). Additionally, permutation multivariate analysis of variance (PERMANOVA) confirmed significant differences ($P = 0.001$) in beta diversity between infected and uninfected groups, with infected samples forming unique clusters separate from uninfected controls (Fig. 2B, Table 2).

In order to assess the relationship between degree of viral load, shedding, and microbiota diversity, correlation analysis was carried out. Results revealed that higher oral viral loads and cloaca viral shedding are strongly associated ($P < 0.001$) with lower Shannon diversity at d3 pi (Fig. 3). The correlation between beta diversity (PERMANOVA models), viral load, and viral shedding was not statistically significant (Supplementary Fig. S2). However, d3 pi showed the highest positive correlation with viral shedding, suggesting a potential association at this time point. Internal sample alpha diversity was estimated using the number of observed features (richness). Rarefaction curves of observed features reached a plateau in all samples, demonstrating that sequencing depth was adequate to cover bacterial diversity in all samples (Supplementary Fig. S3).

AIV H9N2 infection induces differential microbial composition.

Sequencing of the 16S rRNA V4–V5 region generated 1 917 894 quality reads, averaging 26 637 reads per sample after quality filtering and demultiplexing. A total of 573 operational taxonomic units (OTUs) were identified at a 97% sequence similarity level across all samples.

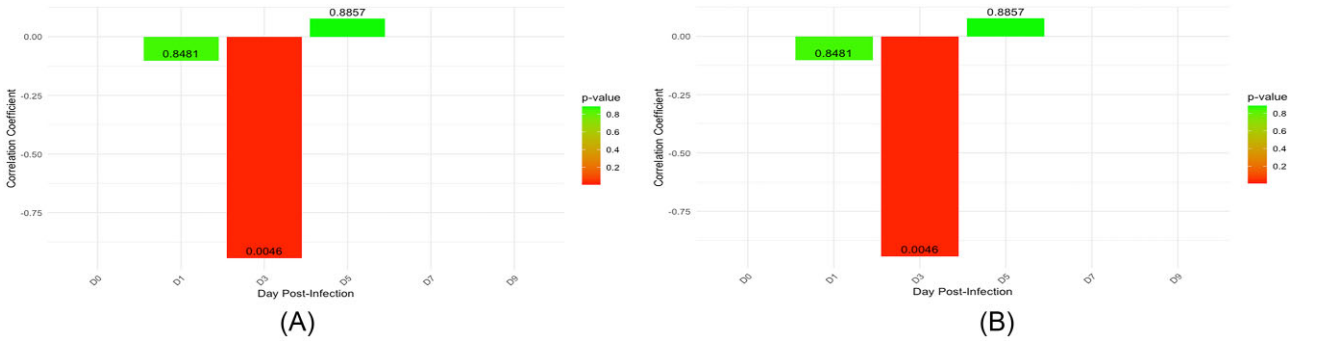

Figure 3. Correlation results between Alpha diversity index: Shannon diversity and viral metrics. (A) Shannon diversity and viral shedding (Log_{10} $TCID_{50}$ ml cloaca). (B) Shannon diversity and viral load (Log_{10} $TCID_{50}$ ml oral). The bar plots display Pearson correlation coefficients for each metric. Colors indicate *P*-values, with red representing higher *P*-values and green representing lower p-values.

The top three predominant phyla identified were Actinobacteria, Firmicutes, and Proteobacteria, with their relative abundances depicted in Figs. 4 and 5. Actinobacteria dominated at d0-d3 pi, constituting 70%–75% of the microbiota, decreasing to 6%–10% at d5-d9. Conversely, Proteobacteria exhibited an increasing trend from 10%–12% at d0–d3 to 80%–85% at d5–d9. Firmicutes ranged from 3% to 15% across the sampling period. Analysis of genus-level taxa revealed distinct shifts in microbial composition across days of AIV infection. The top five predominant genera based on high relative abundances included *Allorhizobium-Pararhizobium*, *Camamonas*, *Dickeya*, *Nocardia*, and *Pandoraea*. Notably, the relative abundance of *Dickeya* increased from 5% to 85% with increasing exposure to AIV d 0 to 9. In addition to these predominant genera, other genera such as *Zymomonas*, *Tepidibacter*, and *Staphylococcus* were also prevalent across both tracheal swabs and BAL samples.

Statistical analysis of microbiota composition using the Statistical Analysis of Metagenomic Profiles (STAMP) software revealed significant alterations in microbiota proportions influenced by AIV H9N2 exposure across both sampled sites (Figs 6 and 7). In the trachea, AIV infection led to a reduction in the proportions of Actinobacteria and Firmicutes on d5, d7, and d9, with a significant reduction in Firmicutes alone on d7, and an accompanying increase in Proteobacteria on all these days ($P > 0.001$). In BAL samples, a significant reduction in Actinobacteria and Firmicutes, accompanied by an increase in Proteobacteria, was observed only on d7 ($P > 0.001$). At the genus level, AIV exposure decreased the proportions of *Nocardia* and *Tepidibacter* on d5, d7, and d9, and *Tepidibacter* alone on d7, while the genus *Dickeya* showed increased abundance on all these days in BAL samples ($P > 0.001$). In tracheal swab samples, the abundance of *Dickeya* increased, and *Nocardia* decreased on d7 and d9, with a similar pattern on d5, alongside a reduction in *Tepidibacter* ($P > 0.001$). At the species level, *Dickeya phage* abundance increased consistently following AIV exposure on d5, d7, and d9 in tracheal swab samples ($P > 0.001$). This was accompanied by a reduction in *Streptomyces* sp. on d5 and d9 ($P > 0.001$). In BAL samples, the increased abundance of *Dickeya phage* and reduction in *Streptomyces* sp. were also consistently observed on d5, d7, and d9 following AIV exposure ($P > 0.001$).

AIV H9N2 infection induces peak expression of Type-I interferon (IFN-β) at d5 pi

Elevated transcriptional upregulation of immunoregulatory genes associated with antiviral host defense was observed in the tracheal tissues of AIV H9N2 infected birds (Fig. 8). Specifically, the viral infection triggered high-level expression ($P \leq 0.05$) expression of type-I interferon (IFN-β) at d5 pi compared to the pre-infection level (Fig. 8C). Similarly, expression of the other antiviral gene, viperin, reached the peak d5 pi ($P = 0.01$) compared to the pre-infection level (Fig. 8A).

Discussion

AIVs primarily replicate in epithelial cells of the respiratory and intestinal mucosae, which interact closely with commensal microbiota (Ngunjiri et al. 2019, Taylor et al. 2020). These microbial communities can influence viral infections by either enhancing or inhibiting them (Wilks and Golovkina 2012). While the role of intestinal microbiota in AIV pathogenesis is well-studied (Yitbarek et al. 2018a, b, 2018c), the impact of respiratory microbiota remains less understood. Evidence from mouse and human studies indicates that commensal microbiota may protect against influenza virus infections (Ichinohe et al. 2011, Budden et al. 2017), though the mechanisms are not fully clear. In a bid to address this knowledge gap, this study investigates changes in the URT and LRT microbiota and host immune response following AIV H9N2 infection.

In the present study, the effectiveness of our AIV challenge model was confirmed, our model demonstrated peak infection and viral shedding at day 3 pi, with viral clearance by day 5 pi. Oral and cloacal swabs from uninfected birds tested negative for the virus, aligning with similar studies (Yitbarek 2018b et al. 2018b, Iqbal et al. 2013, Ruiz-Hernandez et al. 2016, Singh et al. 2016). The pattern of infection and shedding indicates strain-specific replication dynamics. Viral infections can alter host microbiota, leading to changes in microbial diversity (Yitbarek et al. 2018a, Li et al. 2018, Wen et al. 2018, Zhao et al. 2018). AIV H9N2 infection reduced alpha diversity (species richness) at days 5, 7, and 9 pi, compared to uninfected controls (d0), with the most significant reduction observed on day 5 pi. Similarly, beta diversity (microbial turnover) also varied with AIV infection. These findings align with previous studies showing decreased microbial diversity in infected chickens (Chrzastek et al. 2021) and swans (Zhao et al. 2018). The decrease in diversity from nares to lungs suggests stronger disruption in upper respiratory sites (Ngunjiri et al. 2021).

The predominant phyla identified were Actinobacteria, Firmicutes, and Proteobacteria, consistent with prior research (Sohail et al. 2015, Ngunjiri et al. 2019, Wang et al. 2022). H9N2 infection led to shifts in microbial populations, including an increase in Proteobacteria and decreases in Actinobacteria and Firmicutes, particularly between days 5–7. This pattern is observed in other models following AIV infection (Yitbarek 2018a et al. 2018a, Deriu et al. 2016, Li et al. 2017, Groves et al. 2018, Khatib et al. 2021). The

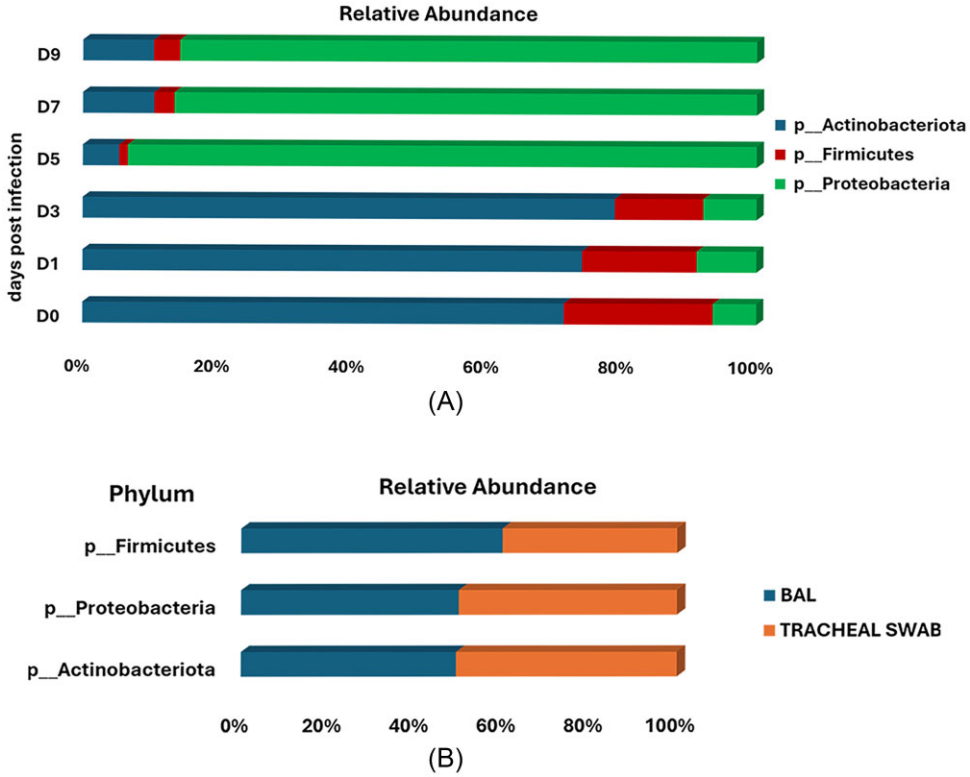

Figure 4. Microbiota profiles of the predominant phyla in the chicken respiratory microbiota, showing (A) variations in H9N2-infected chickens across days 0, 1, 3, 5, 7, and 9 post-infection, and (B) differences between broncho-alveolar lavage (BAL) and tracheal swab samples. Samples were collected pre-challenge (day 0) and at days 1, 3, 5, 7, and 9 post-infection from chickens exposed to 400 μl of 10^7 $TCID_{50}$/ml of H9N2 influenza virus.

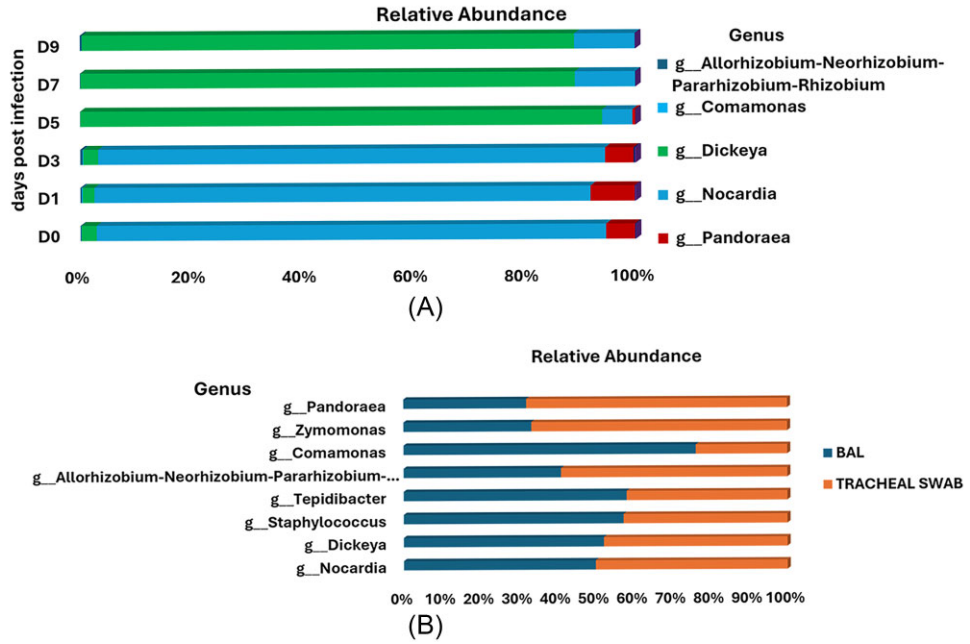

Figure 5. Microbiota profiles of the predominant genera in the chicken respiratory microbiota, showing (A) variations in H9N2-infected chickens across days 0, 1, 3, 5, 7, and 9 post-infection, and (B) differences between broncho-alveolar lavage (BAL) and tracheal swab samples. Samples were collected pre-challenge (day 0) and at days 1, 3, 5, 7, and 9 post-infection from chickens exposed to 400 μl of 10^7 $TCID_{50}$/ml of H9N2 influenza virus.

increased Proteobacteria, associated with inflammation, and decreased Firmicutes and Actinobacteria, important for metabolic and immune functions, suggest microbial dysbiosis.

In terms of microbiota composition, the predominant phyla identified in this study were Actinobacteria, Firmicutes, and Proteobacteria, consistent with previous research (Sohail et al. 2015, Ngunjiri et al. 2019; Wang et al. 2022). Infection with H9N2 AIV in-

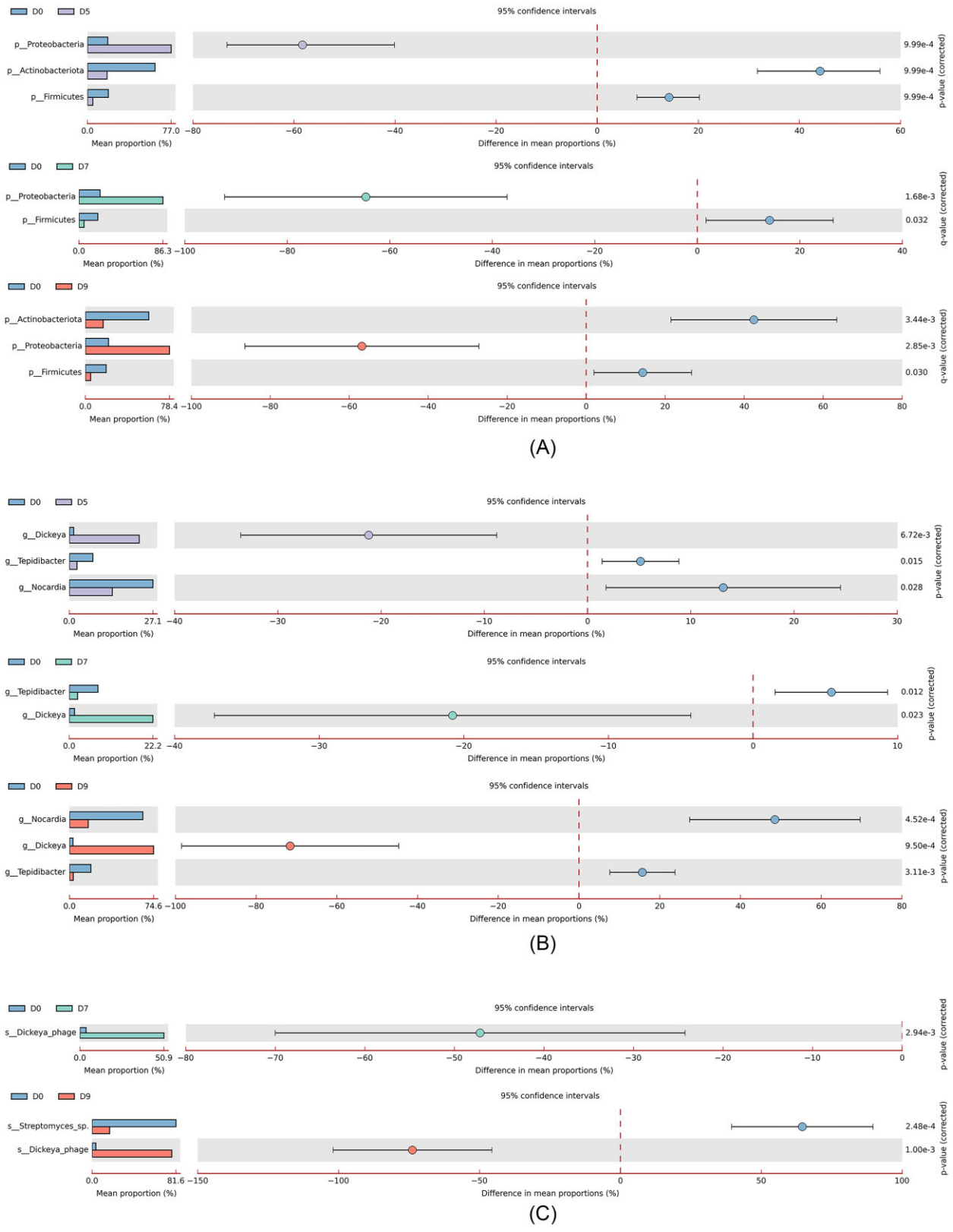

Figure 6. Significant differences ($P < 0.05$) in the cumulative proportions of bacteria at the (A) phylum, (B) genus, and (C) species levels in tracheal swab samples collected from chickens before infection (day 0) and at days 1, 3, 5, 7, and 9 post-infection with H9N2 avian influenza virus. Chickens were inoculated with 400 μl of 10^7 $TCID_{50}$/ml of H9N2 influenza virus.

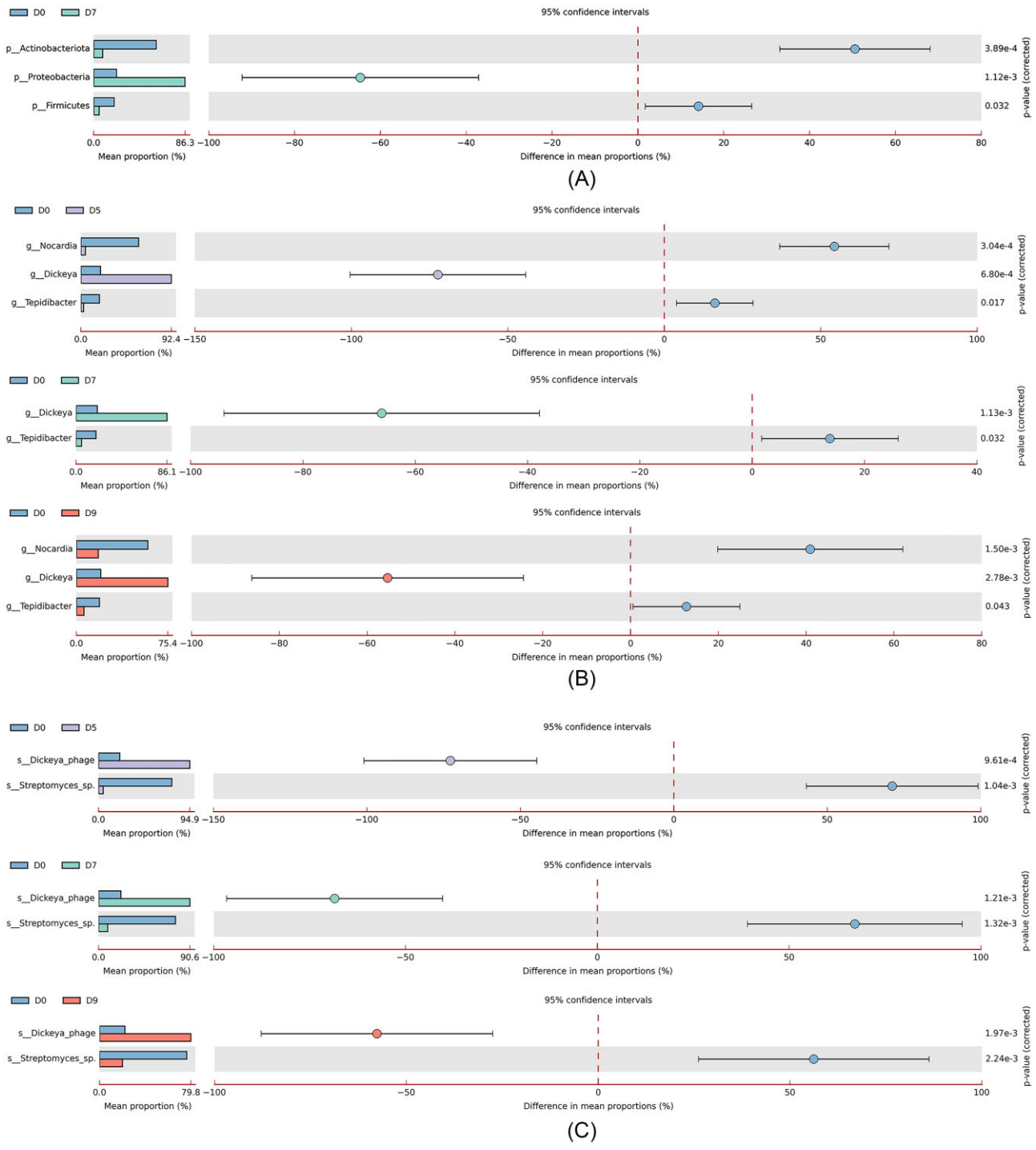

Figure 7. Significant differences ($P < 0.05$) in cumulative bacterial proportions at the (A) phylum, (B) genus, and (C) species levels in BAL samples from chickens infected with H9N2 avian influenza virus (AIV). Samples were collected pre-infection (day 0) and at days 1, 3, 5, 7, and 9 post-infection from chickens inoculated with 400 μl of 10^7 $TCID_{50}$/ml H9N2 influenza virus.

duced shifts in microbial populations at both sampled sites, particularly on d5–d7, which coincided with the time-points recorded with reduced microbial diversity. Specifically blooms of Proteobacteria accompanied by declines in Actinobacteria and Firmicutes abundances were recorded.This pattern is observed in other models following AIV infection (Yitbarek 2018a et al. 2018a, Deriu et al. 2016, Li et al. 2017, Groves et al. 2018, Khatib et al. 2021). Actinobacteria and Firmicutes consist of beneficial Gram-positive species that have diverse metabolic capabilities. Increased Firmicutes populations have been associated with increased nutrient absorption and energy harvest from diets (Jumpertz et al. 2011), while Actinobacteria play a role in combating bacterial diseases and converting feed into microbial biomass (Anandan et al. 2016). The functional roles of these bacterial communities include lipid metabolism and cholesterol metabolism (Martínez et al. 2013), implying that decreases in the microbial population of these groups may impair their functional capacity and overall gut function. On the other hand, increased abundance of Proteobacteria, com-

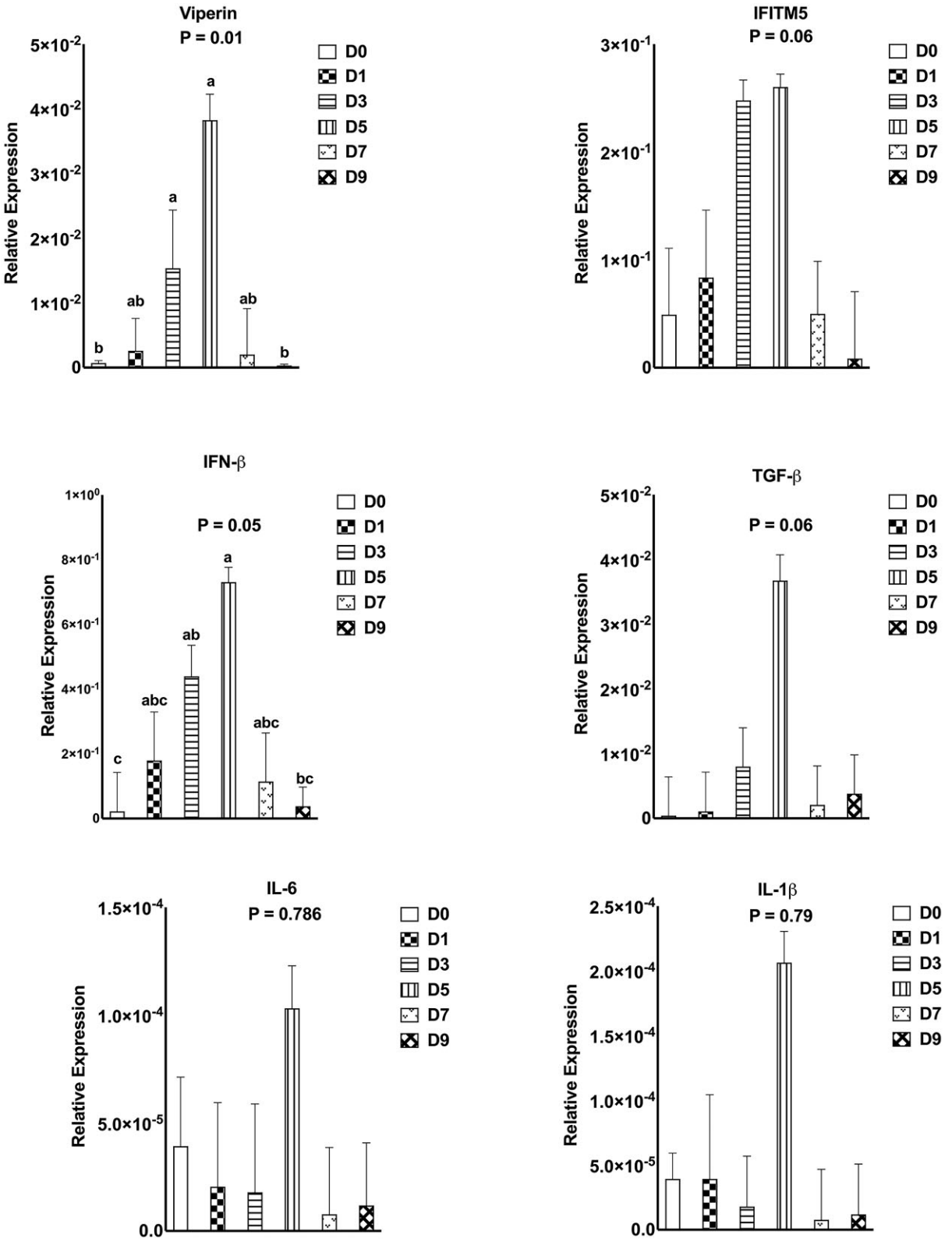

Figure 8. Results of the differential gene expression analysis for (A) Viperin, (B) IFITM5, (C) IFN-β, (D) TGF-β, (E) IL-6, and (F) IL-1-β in H9N2-infected chickens at various time points post-infection (days 0, 1, 3, 5, 7, and 9). Tracheal tissue samples ($n = 8$) were collected before challenge (Day 0) and at Days 1, 3, 5, 7, and 9 post-infection from chickens inoculated with 400 μl of 10^7 TCID50/ml of H9N2 influenza virus. Gene expression levels were measured using real-time PCR and normalized to β-actin. Statistical significance was determined using analysis of variance based on a generalized linear model and Tukey's honest significant difference test, with results presented as means ± standard deviations. Significance was defined as $P \leq 0.05$.

prised primarily of Gram-negative bacteria, are known to be associated with inflammation and metabolic dysfunction (Maharshak et al. 2013, Vaughn et al. 2017). A range of avian pathogens exist in this phylum, including *Escherichia coli*, *Salmonella* spp., and *Campylobacter* spp. An overgrowth of Proteobacteria, particularly *Escherichia coli*, has been reported in several AIV infection studies, suggesting that the increase in Proteobacteria abundance comes at the expense of restricted anaerobic commensals (Wang et al. 2014, Qin et al. 2015, Li et al. 2018). The overgrowth of Proteobacteria following viral infection has also been linked to increased susceptibility to secondary infections and inflammatory pathology (Qin et al. 2015, Li et al. 2018).

Furthermore, during the intermediate of AIV infection (d5–d9), when changes in signs, severity, immune response, and pathogen dynamics may occur, AIV H9N2 led to a decrease in the proportions of *Nocardia* and *Tepidibacter*, along with an increase in *Dickeya* across the sampled sites. *Nocardia* is a genus of aerobic, filamentous, Gram-positive bacteria. *Nocardia* species have been identified as part of dysbiotic intestinal microbiota and associated with prolonged fasting states in some fish species (Kohl et al. 2014, Medina-Felix et al. 2024). Similar to our findings with AIV infection, Wang et al. (2022) reported a significant reduction in *Nocardia* genera in adult zebrafish exposed to aquaculture effluents. While both studies investigate different pathogenic and environmental stressors, the observed changes in microbiome composition, essential for immune responses, indicate alterations in host-microbe interactions due to external stressors, such as viral infection or environmental contamination. The *Tepidibacter* genus consists of thermophilic, Gram-negative anaerobic *Bacteroidetes* bacteria reported as statistically predominant in the respiratory microbiota of healthy pigs, dogs, sheep, and chickens (Zeineldin and Barakat 2023). Lee et al. (2022) reported *Tepidibacter* enrichment in the fecal microbiota of diarrheic cats following *Bacillus licheniformis* fermented product supplementation. While this links *Tepidibacter* abundance to eubiotic microbiota states, further analysis is required to elucidate the metabolic capabilities of this genus. We also recorded increased *Dickeya* genus and *Dickeya phage* abundance post AIV-H9N2 infection at this same timepoint (d5–d9) across both sampled sites, suggesting potential use as a biomarker of AIV-induced poultry respiratory dysbiosis. *Dickeya* are mostly identified as plant pathogens (Samson et al. 2005), with little known regarding their animal metabolic roles. However, Joat et al. (2023) recently identified *Dickeya* as residents of the gut microbiota of commercially raised layer flocks. Increased abundance of this genus has been linked to bacterial microbiomes found in smokeless tobacco, which poses a risk to human oral health, potentially leading to oral tumorigenesis (Vishwakarma et al. 2023). Additionally, increased abundance of the *Dickeya* genus has been linked to obesity in children (Nirmalkar et al. 2018) and fish spoilage (Abdullah et al. 2023). These findings highlight the multifaceted nature of the *Dickeya* genus and their potential impact on host health. In the context of AIV, the elevated presence of *Dickeya* may signify disruptions in the host's microbiome composition, potentially influencing disease progression and host susceptibility. Further studies are needed to validate the association between the *Dickeya* genus and AIV H9N2 infection. At the species level, the present study showed a reduction in the abundance of another beneficial bacterium, *Streptomyces* sp., in both evaluated sites on d5–d9, following AIV H9N2 infection. While the limitation of 16S sequencing technology in terms of sequencing depth at the specie level is acknowledged, the V3V4 hypervariable region have been reported to offer modest taxonomic resolution at an increased cost (Garcia-Lopez et al. 2020, Oladokun et al. 2021). Members of the *Streptomyces* genera are known for producing bioactive secondary metabolites, particularly antibiotics used in medical, agricultural, and veterinary applications (Chater 2006). The probiotic and beneficial effects of *Streptomyces*-derived metabolites have been demonstrated in various models, including in vitro (García-Bernal et al. 2015), invertebrate (Kroiss et al. 2010, Swe et al. 2019, Mazón-Suástegui et al. 2020), and human models (Bolourian and Mojtahedi 2018).

To investigate the mechanism behind AIV H9N2-induced respiratory microbiota dysbiosis in this study, selected cytokine gene expression were quantified. AIV H9N2 is known to replicate efficiently in the trachea compared to other respiratory sites (Ngunjiri et al. 2021). Results revealed a significant increase in IFN-β and viperin gene expression at d5 pi, indicating a peak antiviral response at this time point. This coincided with the lowest microbiota diversity observed in the study. Type-I interferons, including IFN-α and IFN-β, are essential for innate antiviral responses in chickens, inducing an elevated state of anti-viral responses at the cellular level and restricting viral replication processes (McNab et al. 2015). Consistent with previous reports, avian type-I IFNs have been associated with the proliferation of Proteobacteria (Xia et al. 2004, Deriu et al. 2016). Ngunjiri et al. (2021) have demonstrated upregulation of IFN-β in the trachea during H5N2 AIV infection, supporting the current findings. In a mouse model of influenza and bacterial coinfection, Lee et al. (2015) confirmed the crucial role of IFN-β in AIV-induced microbiota dysbiosis. Commensal microbiota normally regulates IFN-β production through transcription factors like c-Jun and NF-kβ, vital for immune homeostasis (Abt et al. 2012). IFN-β production contributes to microbiota dysbiosis by potentially exerting direct antimicrobial effects or indirectly influencing bacterial gene expression. Furthermore, dysregulated IFN-β signaling, commonly observed in chronic infections, could disrupt metabolic pathways, impacting the acquisition of nutrients and metabolites necessary to maintain a balanced microbiota composition (Zhou et al. 2022). The interaction between the influenza A virus and host immune-regulatory factors influences viral growth, with IFN-β and antiviral interferon-stimulated genes (ISGs) playing a key role in the early stage of infection (Ortigoza et al. 2012). As a key downstream anti-viral ISGs, Viperin is greatly expressed in the cells, inducible by both type-I and type-II interferons and is known to inhibit AIV replication (Wang et al. 2007). To this end, our observation of marked expression of the Viperin gene in the birds infected with AIV H9N2, is in line with a previous study where the peakexpression was observed at d5 pi following AIV (H1N1) infection in a murine model (Tan et al. 2012). The transcriptional signals observed, particularly the upregulation of IFN-β and viperin, suggests they likely play a significant role in shaping the respiratory microbiome during H9N2 infection.

Despite the presented results, a few limitations could affect the generalization of the findings. Potential covariates, such as age at the time of sampling and technical variations could influence the observed results. Future studies should consider including these covariates in their analysis to enhance the robustness of similar investigations. While the longitudinal experimental design captures changes over time, is logistically easier to manage, ethically sound, and reduces stress from bird handling, it might have less power to detect individual-level changes over time. To increase the robustness of the investigation, future studies could consider increasing the sample size at each time point. Another potential limitation is the absence of negative extraction controls during the DNA extraction process. While the extraction kit has been validated with sterile PBS as a negative control in previous exper-

iments, the risk of contamination remains in this study. Future research should incorporate validated negative controls to mitigate this risk. Additionally, while this study did not directly analyze the relationship between viral replication and the respiratory microbiota, the observed results on cytokine expression and microbiota diversity suggest a possible interplay. Therefore, further targeted respiratory microbiota manipulation research is needed to directly link these findings and explore the precise mechanisms through which the respiratory microbiota may influence viral replication and immune responses.

Conclusions

The study presented here demonstrated that AIV H9N2 replication in the respiratory tract elicited microbial dysbiosis, evidenced by reduced diversity and the lowest levels observed at 5 days post-infection. In addition to the taxonomic alterations associated with AIV H9N2-induced respiratory dysbiosis, further investigations are warranted to elucidate the functional dysbiotic characteristics of these shifts. Our findings also suggest that AIV H9N2-induced respiratory dysbiosis is facilitated by type-I interferon-mediated mechanisms, particularly through increased IFN-β expression, potentially achieved via direct antimicrobial effects or indirectly through modulation of microbial gene expression or metabolite availability. These effects could subsequently result in elevated expression of interferon-stimulated genes such as viperin. Together, this study supports the hypothesis that chicken respiratory microbiota plays a role in limiting viral replication and initiating anti-influenza immune responses, likely through the modulation of type-I interferon signaling. Therefore, targeted manipulation of the respiratory microbiota might provide additional benefits in controlling avian influenza infections.

Acknowledgment

The authors gratefully acknowledge the staff of the isolation facility at Ontario Veterinary College, University of Guelph, for their assistance in caring for and housing the chickens. Dr Nitish Boodhoo's assistance with figure formatting is greatly appreciated.

Author contributions

Conceptualization—S.S., S.O., M.A.; methodology—S.O., M.A., A.I.M., M.S.D., S.R.; investigation—S.O., M.A., A.I.M., S.R., F.F., J.S., K.B., M.S.D.; formal analysis—S.O., M.A., A.I.M., M.S.D., J.S., S.R.; writing—original draft preparation—S.O.; writing—review & editing—S.S., S.O., M.A., A.I.M., F.F., J.S., K.B., M.S.D., S.R.; funding—S.S. All authors have read and agreed to the published version of the manuscript.

Supplementary data

Supplementary data is available at *FEMSMC Journal* online.

Conflict of interest: Authors declare no conflict of interest.

Funding

This research was partially funded by the Ontario Agri-Food Innovation Alliance, the Canadian Poultry Research Council, and the Ontario Research Fund-Research Excellence.

Data availability

The 16S rRNA gene sequencing data from this study are available at the NCBI repository under BioProject ID PRJNA1104572 and Sequence Read Archive (SRA) submission number SUB14400914, titled 'Avian Influenza and Poultry Microbiome'.

References

Abdullah A, Pratama R, Nurhayati T *et al.* Bacterial community comparison revealed by metagenomic analysis and physicochemical properties of eastern little tuna (Euthynnus affinis) with storage temperature differences. *Fish Aquat Sci* 2023;**26**:593–604.

Abt MC, Osborne LC, Monticelli LA *et al.* Commensal bacteria calibrate the activation threshold of innate antiviral immunity. *Immunity* 2012;**37**:158–70.

Alizadeh M, Shojadoost B, Astill J *et al.* Effects of in ovo inoculation of multi-strain Lactobacilli on cytokine gene expression and antibody-mediated immune responses in chickens. *Front Vet Sci* 2020;**7**:105.

Anandan R, Dharumadurai D, Manogaran GP. An introduction to actinobacteria. In: *Actinobacteria-basics and biotechnological applications*. IntechOpen, Rijeka, 2016.

Barjesteh N, Shojadoost B, Brisbin JT *et al.* Reduction of avian influenza virus shedding by administration of toll-like receptor ligands to chickens. *Vaccine* 2015;**33**:4843–9.

Bolourian A, Mojtahedi Z. Immunosuppressants produced by Streptomyces: evolution, hygiene hypothesis, tumour rapalog resistance and probiotics. *Environ Microbiol Rep* 2018;**10**:123–6.

Boodhoo N, Matsuyama-Kato A, Raj S *et al.* Effect of pre-treatment with a recombinant chicken interleukin-17a on vaccine induced immunity against a very virulent Marek's disease virus. *Viruses* 2023;**15**:1633.

Budden KF, Gellatly SL, Wood DL *et al.* Emerging pathogenic links between microbiota and the gut–lung axis. *Nat Rev Micro* 2017;**15**:55–63.

Cardona CJ, Xing Z, Sandrock CE *et al.* Avian influenza in birds and mammals. *Compar Immunol Microbiol Infect Dis* 2009;**32**:255–73.

Chater KF. Streptomyces inside-out: A new perspective on the bacteria that provide us with antibiotics. *Philos Trans R Soc Lond B Biol Sci* 2006;**361**:761–8.

Chrzastek K, Leng J, Zakaria MK *et al.* Low pathogenic avian influenza virus infection retards colon microbiota diversification in two different chicken lines. *Anim Microbiome* 2021;**3**:1–15. https://doi.org/10.1186/s42523-021-00128-x.

Deriu E, Boxx GM, He X *et al.* Influenza virus affects intestinal microbiota and secondary salmonella infection in the gut through type I interferons. *PLoS Pathog* 2016;**12**:e1005572.

García-Bernal M, Campa-Cordova AI, Saucedo-Lastra PE *et al.* Isolation and in vitro selection of actinomycetes strains as potential probiotics for aquaculture. *Vet World* 2015;**8**:170–6.

García-López R, Cornejo-Granados FA, Lopez-Zavala AA *et al.* Doing more with less: a comparison of 16S hypervariable regions in search of defining the shrimp microbiota. *Microorganisms* 2020;**8**:134.

Groves HT, Cuthbertson L, James P *et al.* Respiratory disease following viral lung infection alters the murine gut microbiota. *Front Immunol* 2018;**9**:182.

Huang SW, Wang SF. The effects of genetic variation on H7N9 avian influenza virus pathogenicity. *Viruses* 2020;**12**:1220.

Ichinohe T, Pang IK, Kumamoto Y *et al.* Microbiota regulates immune defense against respiratory tract influenza A virus infection. *Proc Natl Acad Sci USA* 2011;**108**:5354–9.

Iqbal M, Yaqub T, Mukhtar N *et al.* Infectivity and transmissibility of H9N2 avian influenza virus in chickens and wild terrestrial birds. *Vet Res* 2013;**44**:1–10.

Joat N, Bajagai YS, Van TTH *et al.* The temporal fluctuations and development of faecal microbiota in commercial layer flocks. *Anim Nutr* 2023;**15**:197–209.

Jumpertz R, Le DS, Turnbaugh PJ *et al.* Energy-balance studies reveal associations between gut microbes, caloric load, and nutrient absorption in humans. *Am J Clin Nutr* 2011;**94**:58–65.

Khatib HA, Mathew S, Smatti MK *et al.* Profiling of intestinal microbiota in patients infected with respiratory influenza A and B viruses. *Pathogens* 2021;**10**:761.

Kohl KD, Amaya J, Passement CA *et al.* Unique and shared responses of the gut microbiota to prolonged fasting: A comparative study across five classes of vertebrate hosts. *FEMS Microbiol Ecol* 2014;**90**:883–94.

Kroiss J, Kaltenpoth M, Schneider B *et al.* Symbiotic streptomycetes provide antibiotic combination prophylaxis for wasp offspring. *Nat Chem Biol* 2010;**6**:261–3.

Lee B, Robinson KM, McHugh KJ *et al.* Influenza-induced type I interferon enhances susceptibility to gram-negative and gram-positive bacterial pneumonia in mice. *Am J Physiol Lung Cell Mol Physiol* 2015;**309**:L158–67.

Lee TW, Chao TY, Chang HW *et al.* The effects of Bacillus licheniformis—fermented products on the microbiota and clinical presentation of cats with chronic diarrhea. *Animals* 2022;**12**:2187.

Li H, Liu X, Chen F *et al.* Avian influenza virus subtype H9N2 affects intestinal microbiota, barrier structure injury, and inflammatory intestinal disease in the chicken ileum. *Viruses* 2018;**10**.270

Li Y, Ding J, Xiao Y *et al.* 16S rDNA sequencing analysis of upper respiratory tract flora in patients with influenza H1N1 virus infection. *Front Lab Med* 2017;**1**:16–26.

Lu Y, Zhou G, Ewald J *et al.* MicrobiomeAnalyst 2.0: comprehensive statistical, functional and integrative analysis of microbiome data. *Nucleic Acids Res* 2023.**51** W310–W318

Maharshak N, Packey CD, Ellermann M *et al.* Altered enteric microbiota ecology in interleukin 10-deficient mice during development and progression of intestinal inflammation. *Gut Microbes* 2013;**4**:316–24.

Man WH, de Steenhuijsen Piters WAA, Bogaert D. The microbiota of the respiratory tract: gatekeeper to respiratory health. *Nat Rev Micro* 2017;**15**:259–70.

Martínez I, Perdicaro DJ, Brown AW *et al.* Diet-induced alterations of host cholesterol metabolism are likely to affect the gut microbiota composition in hamsters. *Appl Environ Microb* 2013;**79**:516–24.

Mazón-Suástegui JM, Salas-Leiva JS, Medina-Marrero R *et al.* Effect of Streptomyces probiotics on the gut microbiota of Litopenaeus vannamei challenged with Vibrio parahaemolyticus. *Microbiol Open* 2020;**9**:e967.

McNab F, Mayer-Barber K, Sher A *et al.* Type I interferons in infectious disease. *Nat Rev Immunol* 2015;**15**:87–103.

Medina-Felix D, Vargas-Albores F, Garibay-Valdez E *et al.* Gastrointestinal dysbiosis induced by Nocardia sp. infection in tilapia. *Compar Biochem Physiol D Genom Proteomics* 2024;**49**:101154.

Nagy A, Mettenleiter TC, Abdelwhab EM. A brief summary of the epidemiology and genetic relatedness of avian influenza H9N2 virus in birds and mammals in the Middle East and North Africa. *Epidemiol Infect* 2017;**145**:3320–33.

Ngunjiri JM, Taylor KJ, Abundo MC *et al.* Farm stage, bird age, and body site dominantly affect the quantity, taxonomic composition, and dynamics of respiratory and gut microbiota of commercial layer chickens. *Appl Environ Microb* 2019;**85**:e03137–18.

Ngunjiri JM, Taylor KJ, Ji H *et al.* Influenza A virus infection in turkeys induces respiratory and enteric bacterial dysbiosis correlating with cytokine gene expression. *PeerJ* 2021;**9**:e11806.

Nirmalkar K, Murugesan S, Pizano-Zárate ML *et al.* Gut microbiota and endothelial dysfunction markers in obese Mexican children and adolescents. *Nutrients* 2018;**10**:2009.

Oladokun S, Clark KF, Adewole DI. Microbiota and transcriptomic effects of an essential oil blend and its delivery route compared to an antibiotic growth promoter in broiler chickens. *Microorganisms* 2022;**10**:861.

Oladokun S, Koehler A, MacIsaac J. *et al.* Bacillus subtilis delivery route: effect on growth performance, intestinal morphology, cecal short-chain fatty acid concentration, and cecal microbiota in broiler chickens. *Poultry Sci* 2021;**100**:100809.

Ortigoza M, Dibben O, Maamary J. *et al.* A novel small molecule inhibitor of influenza A viruses that targets polymerase function and indirectly induces interferon. *PLoS Pathog* 2012;**8**:e1002668.

Pantin-Jackwood M, Swayne D. Pathogenesis and pathobiology of avian influenza virus infection in birds. *Rev Sci Tech (Int Off Epizootics)* 2009;**28**:113–36.

Parks DH, Tyson GW, Hugenholtz P. *et al.* STAMP: statistical analysis of taxonomic and functional profiles. *Bioinformatics* 2014;**30**:3123–4.

Poroyko V, Meng F, Meliton A. *et al.* Alterations of lung microbiota in a mouse model of LPS-induced lung injury. *Am J Physiol Lung Cell Mol Physiol* 2015;**309**:L76–83.

Pu J, Yin Y, Liu J. *et al.* Reassortment with dominant chicken H9N2 influenza virus contributed to the fifth H7N9 virus human epidemic. *J Virol* 2021;**95**:10–1128.

Qin N, Zheng B, Yao J. *et al.* Influence of H7N9 virus infection and associated treatment on human gut microbiota. *Sci Rep* 2015;**5**:14771.

Raj S, Matsuyama-Kato A, Alizadeh M. *et al.* Treatment with toll-like receptor (TLR) ligands 3 and 21 prevents fecal contact transmission of low pathogenic H9N2 avian influenza virus (AIV) in chickens. *Viruses* 2023;**15**:977.

Reed LJ, Muench HA. Simple method of estimating fifty percent endpoints. *Am J Epidemiol* 1938;**27**:493–7.

Rostagno MH. Effects of heat stress on the gut health of poultry. *J Anim Sci* 2020;**98**:skaa090.

Ruiz-Hernandez R, Mwangi W, Peroval M. *et al.* Host genetics determine susceptibility to avian influenza infection and transmission dynamics. *Sci Rep* 2016;**6**:26787.

Russell SL, Gold MJ, Hartmann M. *et al.* Early life antibiotic-driven changes in microbiota enhance susceptibility to allergic asthma. *EMBO Rep* 2012;**13**:440–7.

Rutten EPA, Lenaerts K, Buurman WA. *et al.* Disturbed intestinal integrity in patients with COPD: effects of activities of daily living. *Chest* 2014;**145**:245–52.

Samson R, Legendre JB, Christen R. *et al.* Transfer of Pectobacterium chrysanthemi and Brenneria paradisiaca to the genus Dickeya gen. nov. as Dickeya chrysanthemi comb. nov. and Dickeya paradisiaca comb. nov. and delineation of four novel species. *Int J Syst Evol Microbiol* 2005;**55**:1415–27.

Santhakumar D, Rubbenstroth D, Martinez-Sobrido L. *et al.* Avian interferons and their antiviral effectors. *Front Immunol* 2017;**8**:49.

Singh SM, Alkie TN, Nagy É. *et al.* Delivery of an inactivated avian influenza virus vaccine adjuvanted with poly (D, L-lactic-co-glycolic acid) encapsulated CpG ODN induces protective immune responses in chickens. *Vaccine* 2016;**34**:4807–13.

Sohail MU, Hume ME, Byrd JA. *et al.* Molecular analysis of the caecal and tracheal microbiome of heat-stressed broilers supplemented with prebiotic and probiotic. *Avian Pathol* 2015;**44**:67–74.

Suarez DL. Avian influenza: our current understanding. *Anim Health Res Rev* 2010;**11**:19–33.

Swe PM, Zakrzewski M, Waddell R. *et al.* High-throughput metagenome analysis of the Sarcoptes scabiei internal microbiota and in-situ identification of intestinal Streptomyces sp. *Sci Rep* 2019;**9**:11744.

Tan KS, Olfat F, Phoon MC. *et al.* In vivo and in vitro studies on the antiviral activities of viperin against influenza H1N1 virus infection. *J Gen Virol* 2012;**93**:1269–77.

Taylor KJM, Ngunjiri JM, Abundo MC. *et al.* Respiratory and gut microbiota in commercial turkey flocks with disparate weight gain trajectories display differential compositional dynamics. *Appl Environ Microb* 2020;**86**:e00431–20.

Vaughn AC, Cooper EM, DiLorenzo PM. *et al.* Energy-dense diet triggers changes in gut microbiota, reorganization of gut-brain vagal communication, and increases body fat accumulation. *Acta Neurobiol Exp* 2017;**77**:18.

Vishwakarma A, Srivastava A, Mishra S. *et al.* Taxonomic and functional profiling of Indian smokeless tobacco bacteriome uncovers several bacterial-derived risks to human health. *World J Microbiol Biotechnol* 2023;**39**:20.

Wang J, Li FQ, Wei HM. *et al.* Respiratory influenza virus infection induces intestinal immune injury via microbiota-mediated Th17 cell-dependent inflammation. *J Exp Med* 2014;**211**:2397–410.

Wang S, Huang A, Gu Y. *et al.* Rational use of danofloxacin for treatment of Mycoplasma gallisepticum in chickens based on the clinical breakpoint and lung microbiota shift. *Antibiotics* 2022;**11**:403.

Wang X, Hinson ER, Cresswell P. The interferon-inducible protein viperin inhibits influenza virus release by perturbing lipid rafts. *Cell Host Microbe* 2007;**2**:96–105.

Wen Z, Xie G, Zhou Q. *et al.* Distinct nasopharyngeal and oropharyngeal microbiota of children with influenza A virus compared with healthy children. *Biomed Res Int* 2018;**1**:6362716.

WHO. World Health Organization: Avian Influenza: Situation Updates. April 2007. Available from: [http://www.who.int/entity/csr/disease/influenza/H5N1-9reduit.pdf]. Accessed February, 2024

Wilks J, Golovkina T. Influence of microbiota on viral infections. *PLoS Pathog* 2012;**8**:e1002681.

Xia C, Liu J, Wu ZG. *et al.* The interferon-alpha genes from three chicken lines and its effects on H9N2 influenza viruses. *Anim Biotechnol* 2004;**15**:77–88.

Yitbarek A, Alkie T, Taha-Abdelaziz K. *et al.* Gut microbiota modulates type I interferon and antibody-mediated immune responses in chickens infected with influenza virus subtype H9N2. *Benef Microbes* 2018a;**9**:417–27.

Yitbarek A, Taha-Abdelaziz K, Hodgins DC. *et al.* Gut microbiota-mediated protection against influenza virus subtype H9N2 in chickens is associated with modulation of the innate responses. *Sci Rep* 2018b;**8**:13189.

Yitbarek A, Weese JS, Alkie TN. *et al.* Influenza A virus subtype H9N2 infection disrupts the composition of intestinal microbiota of chickens. *FEMS Microbiol Ecol* 2018c;**94**:fix165.

Zeineldin M, Barakat R. Host-specific signatures of the respiratory microbiota in domestic animals. *Res Vet Sci* 2023;**164**:105037.

Zhao G, Gu X, Lu X. *et al.* Novel reassortant highly pathogenic H5N2 avian influenza viruses in poultry in China. *PLoS One* 2012;**7**:e46183.

Zhao N, Wang S, Li H. *et al.* Influence of novel highly pathogenic avian influenza A (H5N1) virus infection on migrating whooper swans fecal microbiota. *Front Cell Infect Microbiol* 2018;**8**:46.

Zhou X, Baumann R, Gao X. *et al.* Gut microbiome of multiple sclerosis patients and paired household healthy controls reveal associations with disease risk and course. *Cell* 2022;**185**:3467–86.

Wang S, 2022 Antibiotics 403, 10.3390/antibiotics11030403, 2079-6382

Received 10 May 2024; **revised** 10 December 2024; **accepted** 2 February 2025